

# Reaction Chemistry & Engineering

Bridging the gap between chemistry and chemical engineering

[rsc.li/reaction-engineering](https://rsc.li/reaction-engineering)

The Royal Society of Chemistry is the world's leading chemistry community. Through our high impact journals and publications we connect the world with the chemical sciences and invest the profits back into the chemistry community.

## IN THIS ISSUE

ISSN 2058-9883 CODEN RCEEBW 9(12) 3063–3320 (2024)



### Cover

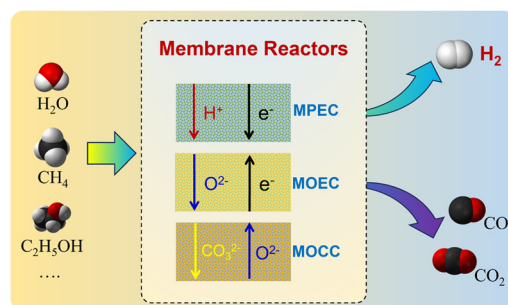
See Kwihwan Kobayashi,  
Nagatoshi Koumura *et al.*,  
pp. 3116–3121.  
Image reproduced by permission  
of Kwihwan Kobayashi from  
*React. Chem. Eng.*, 2024, 9,  
3116.

## REVIEW

3072

### Mixed-conducting ceramic membrane reactors for hydrogen production

Jingjing Tong, Peng Zhang,\* Fuwei Zhuang,  
Yanyan Zheng, Binyan Liu, Xiangping Qiao  
and Xuefeng Zhu\*



## PERSPECTIVE

3100

### ChemPren: a new and economical technology for conversion of waste plastics to light olefins

Anne Gaffney,\* Debtanu Maiti, Debasish Kuila  
and Gennaro Mafia





# Advance your career in science

with professional recognition that showcases your **experience, expertise and dedication**

## Stand out from the crowd

Prove your commitment to attaining excellence in your field

## Gain the recognition you deserve

Achieve a professional qualification that inspires confidence and trust

## Unlock your career potential

Apply for our professional registers (RSci, RSciTech) or chartered status (CChem, CSci, CEnv)

## Apply now

[rsc.li/professional-development](https://rsc.li/professional-development)

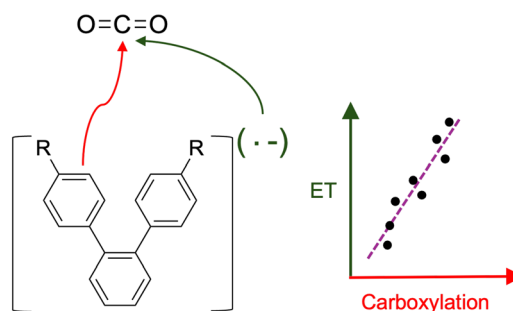


## COMMUNICATIONS

3105

## Linear scaling relationships in homogeneous photoredox catalysis

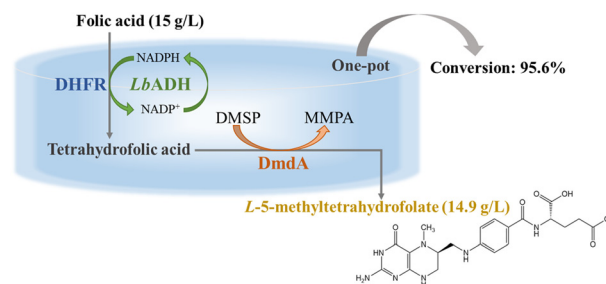
Kareesa J. Kron and Shaama Mallikarjun Sharada\*



3110

## One-pot enzymatic synthesis of L-5-methyltetrahydrofolate from folic acid using enzyme cascades

Linjiang Zhu, Yuxin Wang, Linyan Pan, Enyong Lin, Jiayan Wang and Xiaolong Chen\*

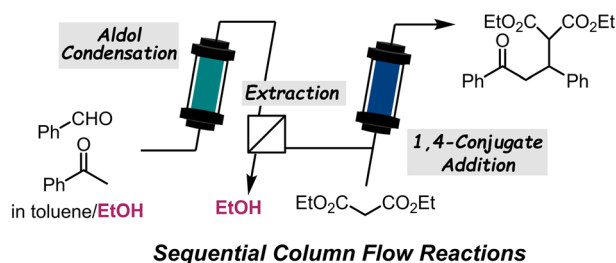


## PAPERS

3116

## Continuous-inline extraction of polar co-solvent during sequential flow reactions

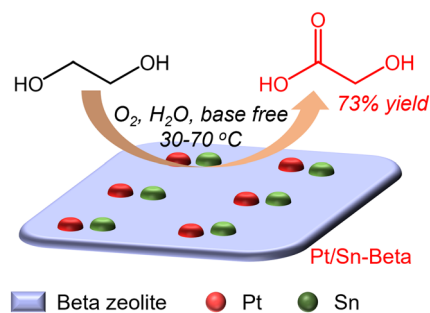
Kwhiwan Kobayashi,\* Jun Matsuzawa, Hajime Kawanami and Nagatoshi Koumura\*



3122

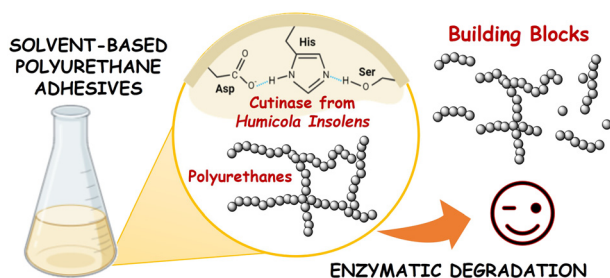
## Synthesis of glycolic acid by selective oxidation of ethylene glycol over Pt/Sn-Beta in a base-free medium

Yongming Xu, Wenzhao Liu, Bo Xu, Ke Wang, Jinchu Yang, Yueqi Si, Xuebin Zhao, Tingting Zhang, Zhan Zhang, Xueyi Qiao\* and Tianliang Lu\*



## PAPERS

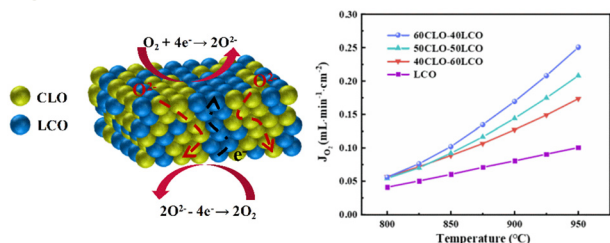
3133



### Enzyme-catalyzed polyurethane adhesive degradation

Angela Romano, Antonella Rosato, Laura Sisti,\*  
Giulio Zanaroli, Svajus Joseph Asadauskas,  
Paulina Nemaniūtė, Dalia Bražinskienė,  
Asta Grigučevičienė and Grazia Totaro

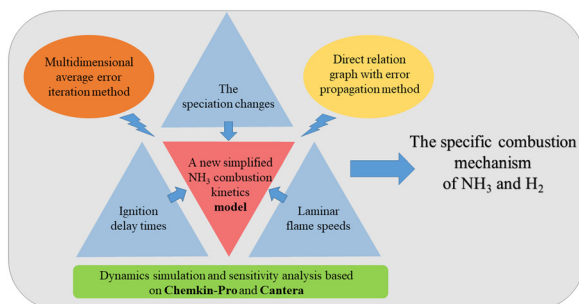
3146



### A mixed ionic and electronic conducting dual-phase oxygen permeable membrane with high CO<sub>2</sub> tolerance

Yihong Xu, Hengcheng Zhu, Song Lei, Zihua Wang  
and Jian Xue\*

3153

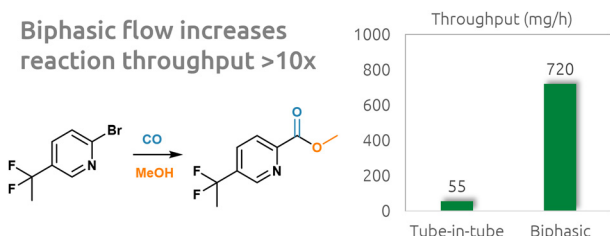


### A simplified chemical kinetic model with a reaction mechanism based on a multidimensional average error iteration method for ammonia and ammonia/hydrogen combustion

Daiyao Yue, Chongkai Zhao, Rui Sun, Jieyu Jiang,  
Chunjie Sui, Xin Zhong and Bin Zhang\*

3172

### Biphasic flow increases reaction throughput >10x



### Carbonylations in flow: tube-in-tube reactor vs. gas-liquid slug flow

Agnieszka Ładosz, Astrid Friedli, Arnaud Lhuillery  
and Georg Rueedi\*

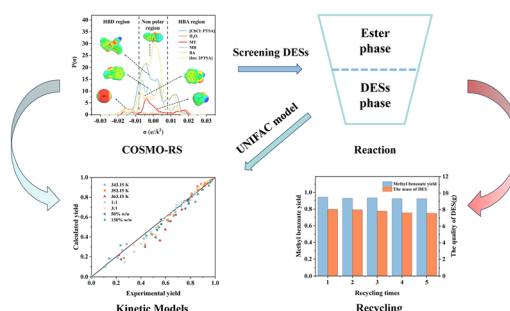


## PAPERS

3179

# Synthesis of methyl benzoate intensified by *p*-toluenesulfonic acid-based deep eutectic solvents

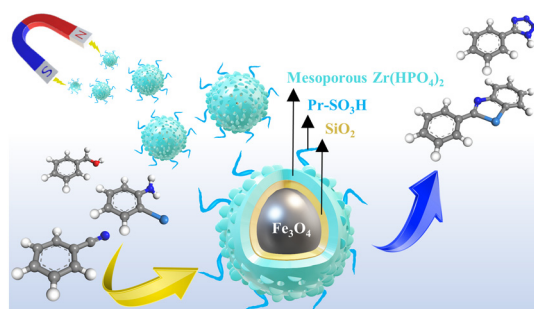
Dian Jin, Xindi Feng, Li Sun,\* Zuoxiang Zeng and Zhen Liu\*



3191

# Magnetic mesoporous zirconium phosphate (MMZP-Pr-SO<sub>3</sub>H): a highly efficient and reusable catalyst for sustainable preparation of phenyl tetrazole and 2-substituted benzoazoles

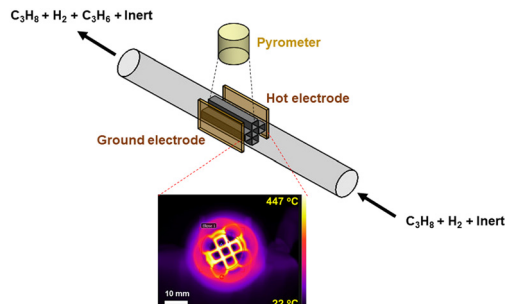
Maryam Tukhani, Abdolreza Hajipour and Alireza Najafi Chermahini\*



3211

# Radio-frequency heating for catalytic propane dehydrogenation

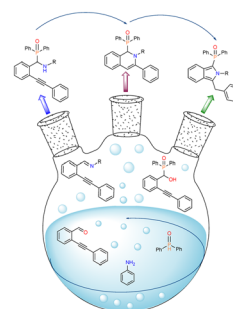
Ankush Rout, Somtochukwu Lambert, Aswin Nair, Kailash Arole, Debalina Sengupta, Mark A. Barteau, Benjamin A. Wilhite\* and Micah J. Green\*



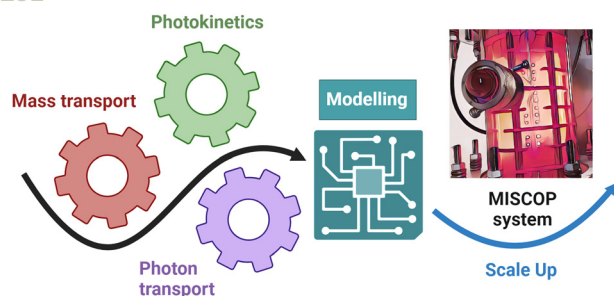
3222

# Synthetic and mechanistic studies of the multicomponent reaction of 2-(phenylethynyl) benzaldehyde, primary amine and diphenylphosphine oxide

Kármén Szabó, Zsolt Kelemen, Pál Tamás Szabó and Erika Bálint\*



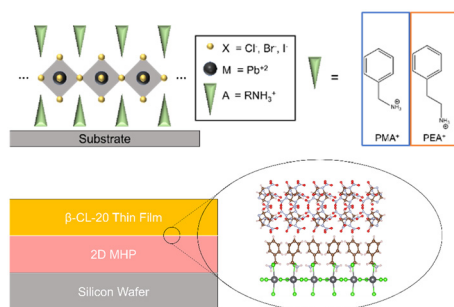
3231



### Modelling the impact of mass transport in a miniplant photoreactor

Florian Gaulhofer, Henning Becker, Alexander Peschl and Dirk Ziegenbalg\*

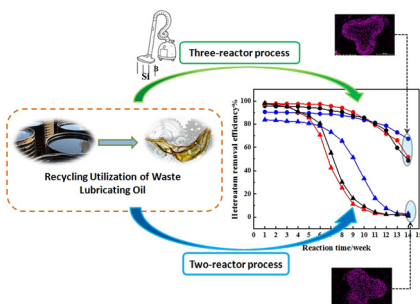
3248



### Utilizing 2D metal halide perovskite thin films as highly tuneable surfaces for orientation control of energetic materials

Natalie Smith-Papin, Meagan Phister, Ashley Conley, Nathan Swami, Zbigniew Dreger and Gaurav Giri\*

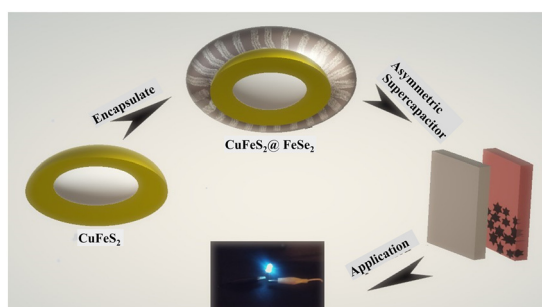
3257



### Application of the three-reactor hydrogenation process in the recycling utilization of waste lubricating oil and study on the catalyst deactivation mechanism

You Fang, Peng Zhang,\* Mengya Guo, Shuke Guo, Fujiang Wang and Mingxing Tang\*

3267



### Spherical CuFeS<sub>2</sub>@FeSe<sub>2</sub> structure as a binder-free electrode and its performance in asymmetric supercapacitors

Tahereh Nikkhah Amirabad\* and Ali A. Ensafi\*





# Selective production of *para*-xylene from biomass-derived 2,5-dimethylfuran through tandem Diels–Alder/dehydration reactions with a bifunctional Ga, Al-zeolite catalyst

Reaction scheme showing the conversion of 2,5-dimethylfuran to 2,5-dimethylbenzene (toluene) using a Ga,Al-BEA zeolite catalyst. The reaction conditions are *n*-heptane, 250°C, 60 bar, 24 h. The catalyst structure is shown as a zeolite framework with Ga<sup>3+</sup> (red dots) and Al<sup>3+</sup> (blue dots) ions. The reaction is highly selective and yields over 57%.

# Syngas production from phenolic pollutants *via* a series of hydroxylation, ring cleavage, and aqueous-phase reforming catalyzed by a hydrotalcite-supported Fe–Mn–Ni alloy

The diagram illustrates the catalytic cycle for the conversion of phenol to tetrahydrofuran (THF) on a Fe-Mn-Ni alloy on hydrotalcite. The cycle involves the following steps:

- Hydroxylation:** Phenol reacts with  $\text{H}_2\text{O}$  and  $\text{Metal Oxide Hydroxide}$  to form a catechol derivative (X) on the catalyst surface.
- Ring Opening:** The catechol derivative (X) undergoes ring opening to form a tetrahydrofuran intermediate.
- Reforming:** The tetrahydrofuran intermediate is reformed to produce  $\text{H}_2$  and  $\text{CO}$ .
- Water-Gas Shift:**  $\text{H}_2$  and  $\text{CO}$  undergo a water-gas shift reaction to produce  $\text{H}_2$  and  $\text{CO}_2$ .
- Octahedral Mineral Formation:**  $\text{H}_2$  and  $\text{CO}_2$  react to form octahedral minerals.
- Strong Lewis Acid Formation:** Octahedral minerals form strong Lewis acids.
- Weak Lewis Acid Formation:** Strong Lewis acids form weak Lewis acids.
- Tetrahydrofuran Mineral Formation:** Weak Lewis acids form tetrahydrofuran minerals.
- Ring Opening:** Tetrahydrofuran minerals undergo ring opening to regenerate the catalyst surface for hydroxylation.

# Flexible carbon fibres with magnetic ZIF-67 as a core layer and *in situ* grown NiMn-LDH nanosheets as a shell layer for microwave absorption

The figure illustrates the synthesis of Co/CF@NiMn-LDH. It begins with the combination of ZIF-67 (a purple polyhedral structure) and PAN (a blue polymer chain). These components are subjected to electrospinning, represented by a syringe and a grounded plate, to create a ZIF-67/CF composite fiber. This fiber then undergoes carbonization, shown as a transition to a solid black cylinder labeled Co/CF. Finally, a solvothermal process, depicted with a reaction vessel, leads to the formation of the final product, Co/CF@NiMn-LDH, which is shown as a green, porous, layered structure. An inset graph plots the Return Loss (RL) in dB against Frequency in GHz for various sample thicknesses: 2.0 mm, 2.2 mm, 2.4 mm, 2.6 mm, 2.8 mm, and 3.8 mm. The graph shows resonance peaks that shift to lower frequencies as the thickness increases. A specific peak for the 2.8 mm sample is highlighted at approximately 8.5 GHz with an RL of -53 dB.

## Application of a simple rule for the design of micro- or meso-scale cooled reactors in a heat transfer limited regime

250 psig back pressure regulator  
 1/2 psi check valve  
 1/2 turn ball valve  
 Gibbon Pumps  
 3 NaOH feed pump  
 Peroxide feed  
 Hydrogen peroxide feed pump  
 Organic feed pump  
 Pressure sensor  
 Insulated water bath  
 Thermocouple  
 Caustic feed  
 Organic feed  
 1/2 copper coil heat exchanger